Archives of Biochemistry and Biophysics 694 (2020) 108615

Contents lists available at ScienceDirect

Archives of Biochemistry and Biophysics

journal homepage: www.elsevier.com/locate/yabbi

Preferential modification of CyaA-hemolysin by CyaC-acyltransferase through the catalytic Ser^{30}-His^{33} dyad in esterolysis of palmitoyl-donor substrate devoid of acyl carrier proteins

Mattayaus Yentongchai [a], Niramon Thamwiriyasati [b,**], Chompounoot Imtong [c], Hui-Chun Li [d], Chanan Angsuthanasombat [a,d,e,*]

[a] Bacterial Toxin Research Innovation Cluster (BRIC), Institute of Molecular Biosciences, Mahidol University, Salaya Campus, Nakornpathom, 73170, Thailand
[b] Molecular Medicine Research Group (MMRG), Division of Medical Technology, Faculty of Allied Health Sciences, Burapha University, Chonburi, 20131, Thailand
[c] Division of Biology, Department of Science, Faculty of Science and Technology, Prince of Songkla University, Pattani, 94000, Thailand
[d] Department of Biochemistry, School of Medicine, Tzu Chi University, Hualian, 97004, Taiwan
[e] Laboratory of Synthetic Biophysics and Chemical Biology, Biophysics Institute for Research and Development (BIRD), Chiang Mai, 50230, Thailand

ARTICLE INFO

Keywords:
CyaC-acyltransferase
Esterolysis
A nucleophile activation dyad
Palmitoylation
p-Nitrophenyl derivatives
Toxin activation

ABSTRACT

We previously demonstrated that the ~130-kDa CyaA-hemolysin domain (CyaA-Hly) from *Bordetella pertussis* co-expressed with CyaC-acyltransferase in *Escherichia coli* was acylated at Lys^{983} and thus activated its hemolytic activity. Here, attempts were made to provide greater insights into such toxin activation *via* fatty-acyl modification by CyaC-acyltransferase. Non-acylated CyaA-Hly (NA/CyaA-Hly) and CyaC were separately expressed in *E. coli* and subsequently purified by FPLC to near homogeneity. When effects of acyl-chain length were comparatively evaluated through CyaC-esterolysis using various *p*-nitrophenyl (pNP) derivatives, Michaelis-Menten steady-state kinetic parameters (K_M and k_{cat}) of CyaC-acyltransferase revealed a marked preference for myristoyl ($C_{14:0}$) and palmitoyl ($C_{16:0}$) substrates of which catalytic efficiencies (k_{cat}/K_M) were roughly the same (~1.5×10^3 $s^{-1}mM^{-1}$). However, pNP-palmitate (pNPP) gave the highest hemolytic activity of NA/CyaA-Hly after being acylated *in vitro* with a range of acyl-donor substrates. LC-MS/MS analysis confirmed such CyaC-mediated palmitoylation of CyaA-Hly occurring at Lys^{983}, denoting no requirement of an acyl carrier protein (ACP). A homology-based CyaC structure inferred a role of a potential catalytic dyad of conserved Ser^{30} and His^{33} residues in substrate esterolysis. CyaC-ligand binding analysis *via* molecular docking corroborated high-affinity binding of palmitate with its carboxyl group oriented toward such a dyad. Ala-substitutions of each residue (S30A or H33A) caused a drastic decrease in k_{cat}/K_M of CyaC toward pNPP, and hence its catalytic malfunction through palmitoylation-dependent activation of NA/CyaA-Hly. Altogether, our present data evidently provide such preferential palmitoylation of CyaA-Hly by CyaC-acyltransferase through the enzyme Ser^{30}-His^{33} nucleophile-activation dyad in esterolysis of palmitoyl-donor substrate, particularly devoid of a natural acyl-ACP donor.

1. Introduction

Bordetella pertussis, a Gram-negative pathogenic bacterium that causes whooping cough (also known as 'pertussis'), secretes the bi-functional adenylate cyclase (AC)-hemolysin (Hly) toxin (CyaA) which harbors both calmodulin-dependent AC and hemolytic/pore-forming activities [1,2]. Whooping cough which is a highly contagious respiratory tract infection in humans has re-emerged globally as a consequence of declining immunity, following vaccination and imperfect vaccination of populations [3–5], hence requiring new approches for effective treatment of such a re-emerging infectious disease. We recently generated CyaA-specific humanized VH/V_HH nanobodies that would have promising applications in potential development of a novel anti-pertussis agent [6].

* Corresponding author. Bacterial Toxin Research Innovation Cluster (BRIC), Institute of Molecular Biosciences, Mahidol University, Salaya Campus, Nakornpathom, 73170, Thailand.
** Corresponding author.
E-mail addresses: niramon@go.buu.ac.th (N. Thamwiriyasati), chanan.ang@mahidol.ac.th (C. Angsuthanasombat).

https://doi.org/10.1016/j.abb.2020.108615
Received 10 June 2020; Received in revised form 4 September 2020; Accepted 29 September 2020
Available online 2 October 2020
0003-9861/

The ~180-kDa CyaA toxin preferentially binds to the $\alpha_M\beta_2$ integrin (CD11b/CD18) of macrophages [7] that will enable entry of its AC catalytic domain into the cell to induce apoptosis toward intracellular accumulation of cyclic AMP [8]. Recently, this key virulence factor−CyaA has been shown to bind to an inactive form of an integrin called complement receptor 3 (CR3) residing on the surface of many immune cells, enabling the toxin to use the integrin without triggering an immune response [9]. Nonetheless, CyaA also causes hemolysis of sheep erythrocytes lacking the intergrin receptor [10], thus suggesting an alternative mechanism of target cell binding. Moreover, the ~130-kDa truncated CyaA fragment, termed CyaA-Hly, retains hemolytic activity independent of the N-terminal AC domain [11] and can also induce ion-channel formation in receptor-free planar lipid bilayers [12]. Particularly, positively-charged side-chains in the pore-lining helix 3 were demonstrated to be important for hemolytic activity and ion-channel opening of CyaA-Hly [13].

CyaA which belongs to the RTX (Repeat-in-ToXin) cytolysin family is initially produced as inactive proCyaA and converted intracellularly to the mature active toxin *via* a post-translational acylation mediated by the endogenous CyaC-acyltransferase [14]. An acyl group predominantly found to be attached to CyaA at Lys^{983} is a $C_{16:0}$-hydrocarbon chain (*i.e.* palmitoyl) [15,16], although the exact role in toxin function of such conjugated palmitoyl is yet unclear. Nonetheless, it was initially proposed that channel-forming activity of the ~180-kDa full-length CyaA toxin was strongly dependent on toxin modification *via* palmitoylation, albeit not yet clear for the involvement of the attached palmitoyl moiety in channel-pore formation [17]. The added palmitoyl moiety was also suggested to increase membrane affinity of the full-length CyaA toxin needed for efficient attachment to the target cell membrane by serving as a membrane-associating mediator or a receptor-toxin interaction determinant [18]. However, our recent studies demonstrated that such toxin modification *via* Lys^{983}-palmitoylation was not essential for binding of the 130-kDa CyaA-Hly domain to target erythrocyte membranes, but rather needed for stabilizing toxin-induced ion-leakage pores [19]. More recently, we have shown that the N-terminal hydrophobic region (Met^{482}-Leu^{750}) of CyaA-Hly is conceivably required for not only membrane-pore formation but also functional association with CyaC-acyltransferase, and hence effective palmitoylation at Lys^{983} [20].

All RTX toxins are conceivably believed to be activated by similar mechanisms despite variations in the location, number and chain length of the conjugated acyl group [21]. However, molecular basis for the substrate specificity and catalytic mechanism of the CyaC-acyltransferase is not clearly defined. In our previous studies, we demonstrated that the recombinant CyaC-acyltransferase, which was effectively refolded after urea solubilization, was able to activate the 130-kDa non-acylated CyaA-Hly (NA/CyaA-Hly) fragment in the presence of *E. coli* lysate containing ACPs to become hemolytically active [22]. In this study, to gain more critical insights into the molecular mechanism of CyaC catalysis, we have successfully devised an *in vitro* activation system for NA/CyaA-Hly toward pNP derivatives as mimics of the natural acyl-ACP donor. Moreover, structural analysis of CyaC *via* protein-ligand docking together with mutagenesis results revealed a critical role of a potential catalytic dyad of conserved Ser^{30} and His^{33} residues in substrate esterolysis for toxin activation through preferential palmitoylation at Lys^{983}.

2. Materials and methods

2.1. Construction of CyaC mutants via site-directed mutagenesis

The pCyaC plasmid encoding the ~21-kDa CyaC-acyltransferase [23] was used as a template for single-alanine substitutions at Ser^{30} and His^{33} performed by PCR-based directed mutagenesis using a high fidelity Phusion DNA polymerase (Finnzymes, Finland), following the Quick-Change Mutagenesis Kit (Stratagene) as previously described [22]. Complementary pairs of mutagenic primers were designed based on the cloned *cyaC* gene sequence (*see* Supplementary Table S1). Mutant plasmids were first identified by restriction endonuclease digestion and subsequently verified by DNA sequencing.

2.2. Protein preparations of CyaC wild-type and its mutants

CyaC wild-type and its mutants were over-expressed in *E. coli* BL21 (DE3)pLysS under control of the IPTG-inducible *T7* promoter as described previously [23]. After harvested by centrifugation, *E. coli* cells expressing each individual CyaC protein as inclusions were resuspended in 20 mM Tris-HCl (pH 8.0) and disrupted by using a French Pressure Cell (10,000 psi). Insoluble inclusions separated from crude lysate by centrifugation (12,000×*g*, 20 min) were solubilized in 20 mM Tris-HCl (pH 8.0) containing 8 M urea for 1 h. Unfolded CyaC proteins were initially refolded in a low [urea]-refolding buffer (20 mM Tris-HCl, pH 8.0, 150 mM NaCl, 2 M urea) for 4 h and finally dialyzed twice against the same buffer without urea for 4 h [22]. The refolded proteins were then subjected to size-exclusion chromatography (SEC, Superdex™ 75, GE Healthcare) equilibrated with 20 mM Tris-HCl (pH 8.0), 150 mM NaCl, and the eluted factions were analyzed by SDS-PAGE (sodium dodecyl sulfate-polyacrylamide gel electrophoresis).

2.3. Expression and purification of soluble non-acylated CyaA-Hly

CyaA-Hly was expressed without CyaC-acyltransferase (termed non-acylated CyaA-Hly, NA/CyaA-Hly) in *E. coli* BL21(DE3)pLysS under control of the *T7* promoter as described previously [23]. The cultured cells were harvested by centrifugation, resuspended in 20 mM Tris-HCl (pH 8.0) containing 5 mM $CaCl_2$ and 1 mM PMSF (phenylmethylsulfonyl fluoride) and disrupted in a French Pressure Cell. After centrifugation (12,000×*g*, 20 min), the soluble NA/CyaA-Hly protein in the lysate supernatant was sequentially purified by anion-exchange chromatography (AEC, HiTrap Q HP, GE Healthcare) and SEC (Superose® 12, GE Healthcare), and the purified protein was analyzed by SDS-PAGE.

2.4. CyaC-esterolytic activity assays toward p-nitrophenyl (pNP) derivatives

Esterolytic activity of CyaC-acyltransferase (15 μg/mL or ~0.7 μM) was assayed toward a number of pNP derivatives, *i.e.*, *p*-nitrophenyl acetate (pNPA, $C_{2:0}$), *p*-nitrophenyl carpyrate (pNPC, $C_{8:0}$), *p*-nitrophenyl decanoate (pNPD, $C_{10:0}$), *p*-nitrophenyl myristate (pNPM, $C_{14:0}$), *p*-nitrophenyl palmitate (pNPP, $C_{16:0}$) and *p*-nitrophenyl stearate (pNPS, $C_{18:0}$) dissolved in isopropanol. The CyaC-catalyzed reaction was performed in 50 mM Tris-HCl (pH 7.4) at 25 °C and its enzymatic rate was determined *via* the formation of pNP product by measuring OD_{400} (ε = 11.6 $mM^{-1}c^{-1}$) [24] with SoftMax Pro spectrophotometer (0.7-cm light-path). Steady-state kinetics were recorded by varying concentrations of pNP substrates (10-500 μM) and the corresponding kinetic parameters (V_{max} and K_M) were determined by non-linear fitting of untransformed data to the Michaelis-Menten (M-M) equation by using GraphPad Prism 5 software. Catalytic constant (k_{cat}) and catalytic efficiency (k_{cat}/K_M) were calculated by using the active enzyme concentration.

2.5. Assessment of hemolytic activity of activated CyaA-Hly

In vitro activation of CyaA-Hly was set up by mixing purified NA/CyaA-Hly (10 μg) and purified CyaC (15 μg) together with varying concentrations (10-500 μM) of pNP derivatives in 1 mL of TBS buffer (20 mM Tris-HCl, pH 7.4, 150 mM NaCl, 5 mM $CaCl_2$) and incubated at 37 °C for 5 min. After the activation, 10-μl sheep erythrocytes (10^8 cells/mL) were added to each 1-mL mixture sample and incubated at 37 °C for 5 h. After centrifugation (10,000×*g*, 5 min), erythrocyte lysis was determined by measuring OD_{540} of the supernatant. OD_{540} value

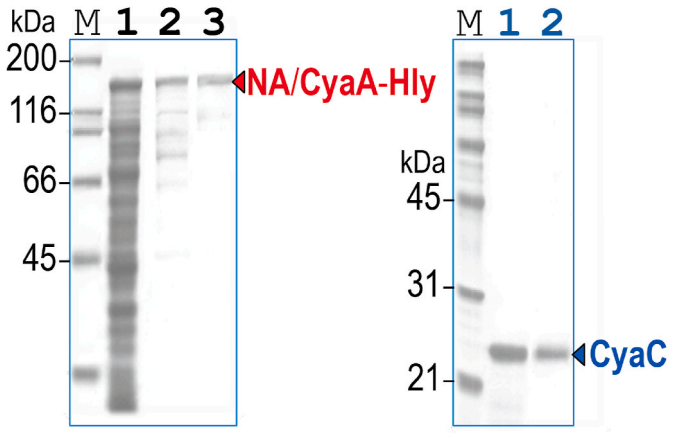

Fig. 1. *Left panel,* SDS-PAGE (Coomassie brilliant blue-stained 12% gel) of NA/CyaA-Hly preparation. Lane 1, crude extracts from *E. coli* cells expressing the 130-kDa NA/CyaA-Hly. Lanes 2 and 3, purified NA/CyaA-Hly obtained by AEC and SEC, respectively. *Right panel,* SDS-PAGE (Coomassie brilliant blue-stained 12% gel) of CyaC preparation. Lane 1, insoluble fraction of crude extracts from *E. coli* cells expressing the 21-kDa CyaC-acyltransferase. Lane 2, SEC-purified CyaC after unfolding-refolding processes. M, molecular mass standards. (For interpretation of the references to color in this figure legend, the reader is referred to the Web version of this article.)

corresponding to complete hemolysis was obtained by lysing the erythrocytes with 0.1% Triton-X 100 while spontaneous hemolysis was determined by incubating the erythrocyte suspensions in buffer alone. Percentage of hemolysis was calculated by [(OD_{540} sample − OD_{540} negative control)/(OD_{540} of 100% hemolysis − OD_{540} negative control)] × 100. For comparison of acylation activities between CyaC wild-type and its mutants, only pNPP with a fixed concentration of 500 μM was used as an acyl-donor substrate.

2.6. Verification of acylated CyaA-Hly via LC-MS/MS analysis

To examine whether there is a presence of palmitate ($C_{16:0}$) at Lys^{983} acylation site of CyaA-Hly mediated by CyaC or its mutants, such CyaA-Hly protein bands resolved by SDS-PAGE were excised and eluted from the gel prior to digestion with trypsin according to a standard protocol. LC-MS/MS (liquid chromatography-tandem mass spectrometry, Finnigan LTQ Linear Ion Trap Mass Spectrometer) was used to analyze the purified trypsin-generated peptide fragments.

2.7. Homology-based modeling of CyaC structure

A plausible three-dimensional (3D) CyaC model was generated based on the target-template alignment with the ApxC known structure (PDB-4whn, the 172-amino acid toxin-activating acyltransferase from *Actinobacillus pleuropneumoniae*) [25] *via* SWISS-MODEL homology modeling. As analyzed *via* compositional score matrix adjustment of the NCBI's protein-query protein-database BLAST program, the pairwise sequence alignment between CyaC and ApxC revealed ~39% identity (60/155 residues) and 60% homology (93/155 residues). Coordinates which are conserved between the target and the template were copied from the template to the model. Insertions and deletions were re-modeled using a fragment library. Side chains were then rebuilt and the geometry of the resulting model was finally regularized by using a force field. The global and per-residue model quality was assessed using the QMEAN scoring function [26].

2.8. CyaC-ligand docking

To determine an optimal ligand-binding mode of CyaC for a palmitate, the ligand (free palmitic acid) was docked *in silico* into a potential binding site of the CyaC modeled structure using SwissDock, an EADock DSS-based web server (http://www.swissdock.ch) dedicated to the docking of a small molecule on a target protein [27]. The resulting docking models were analyzed by using UCSF Chimera and PyMOL.

Table 1
Kinetic parameters for CyaC esterolysis with different acyl chain-length substrates[a].

Substrate	V_{max} (U/mg)[b]	k_{cat} (s^{-1})	K_M (mM)	k_{cat}/K_M (s^{-1} mM^{-1})
pNPA ($C_{2:0}$)	0.50 × 10^2 ± 1.0	0.18 × 10^2 ± 0.2	0.11 ± 0.01	1.7 × 10^2 ± 11
pNPC ($C_{8:0}$)	4.5 × 10^2 ± 9.0	1.6 × 10^2 ± 3.3	0.64 ± 0.02	2.5 × 10^2 ± 4.8
pNPD ($C_{10:0}$)	3.3 × 10^2 ± 4.9	1.1 × 10^2 ± 1.7	0.38 ± 0.01	3.0 × 10^2 ± 2.6
pNPM ($C_{14:0}$)	2.4 × 10^3 ± 96	8.4 × 10^2 ± 33	0.55 ± 0.05	1.5 × 10^3 ± 86
pNPP ($C_{16:0}$)	1.5 × 10^3 ± 26	5.2 × 10^2 ± 9.2	0.34 ± 0.01	1.5 × 10^3 ± 10
pNPS ($C_{18:0}$)	8.6 × 10^2 ± 35	3.0 × 10^2 ± 12	1.4 ± 0.09	2.1 × 10^2 ± 5.3

[a] Results were averaged from three independent experiments. Both M-M and Lineweaver-Burk plots of individual corresponding data are shown in Supplementary Fig. S3.
[b] One unit of enzyme activity is defined as the amount of enzyme liberating 1 μmol of substrates in 1 min at 37 °C.

3. Results and discussion

3.1. Substrate preference of CyaC-acyltransferase analyzed through its esterolytic kinetics

At the start, the ~130-kDa non-acylated form of CyaA-Hly (NA/CyaA-Hly) which was optimally expressed as a soluble protein was sequentially purified by AEC and SEC to near homogeneity as analyzed by SDS-PAGE (Fig. 1, *left panel*). Moreover as shown in Fig. 1 (*right panel*), the recombinant CyaC-acyltransferase which was over-expressed mostly as an insoluble inclusion was completely solubilized in 8M-urea denaturing buffer. The soluble protein after refolding in a low [urea]-refolding buffer was purified *via* SEC which indicated that the urea-free refolded protein was recovered in a single peak containing a >95%-pure band of the ~21-kDa CyaC protein as verified by SDS-PAGE (*see* Fig. 1, *right panel, lane 2*).

To gain more insights into toxin activation through CyaC catalysis, the M-M kinetic parameters, *i.e.*, the maximum reaction rate (Vmax) and the Michaelis constant (K_M), of the enzymatic esterolytic reaction toward various pNP derivatives containing different even-type acyl-chain lengths (short $C_{2:0}$, medium $C_{8:0}$-$C_{10:0}$ and long $C_{14:0}$-$C_{18:0}$) were comparatively determined. As can be seen from Table 1, the longest chain-length (pNPS, $C_{18:0}$) among the varying acyl groups resulted in the highest K_M value (~1.4 mM) for CyaC esterolysis, indicating the lowest affinity of the enzyme toward this stearyl group. The Vmax and catalytic constant (k_{cat}) values of the enzyme appeared to be greatest for the myristoyl (pNPM, $C_{14:0}$) substrate, giving a maximum catalytic efficiency (k_{cat}/K_M) of ~1.5 × 10^3 $s^{-1}mM^{-1}$. It should be noted that this enzyme seemed to exhibit the highest-affinity binding (~K_M value of ~0.1 mM) with the $C_{2:0}$ chain-length acyl group (pNPA), albeit the Vmax and k_{cat} values toward this substrate were lowest (only ~50 U/mg and ~18 s^{-1}, respectively).

Minimal differences in k_{cat} and K_M values were observed between the $C_{14:0}$ and $C_{16:0}$ chain-length substrates, resulting in similar catalytic efficiencies (~1.5 × 10^3 $s^{-1}mM^{-1}$) with both substrates (*see* Table 1). Overall, these kinetic parameters of such CyaC-esterolytic reaction toward various acyl-chain length derivatives consistently revealed an obvious preference for both pNPM ($C_{14:0}$) and pNPP ($C_{16:0}$) as substrates. Our data are in agreement with other kinetic studies of HlyC-

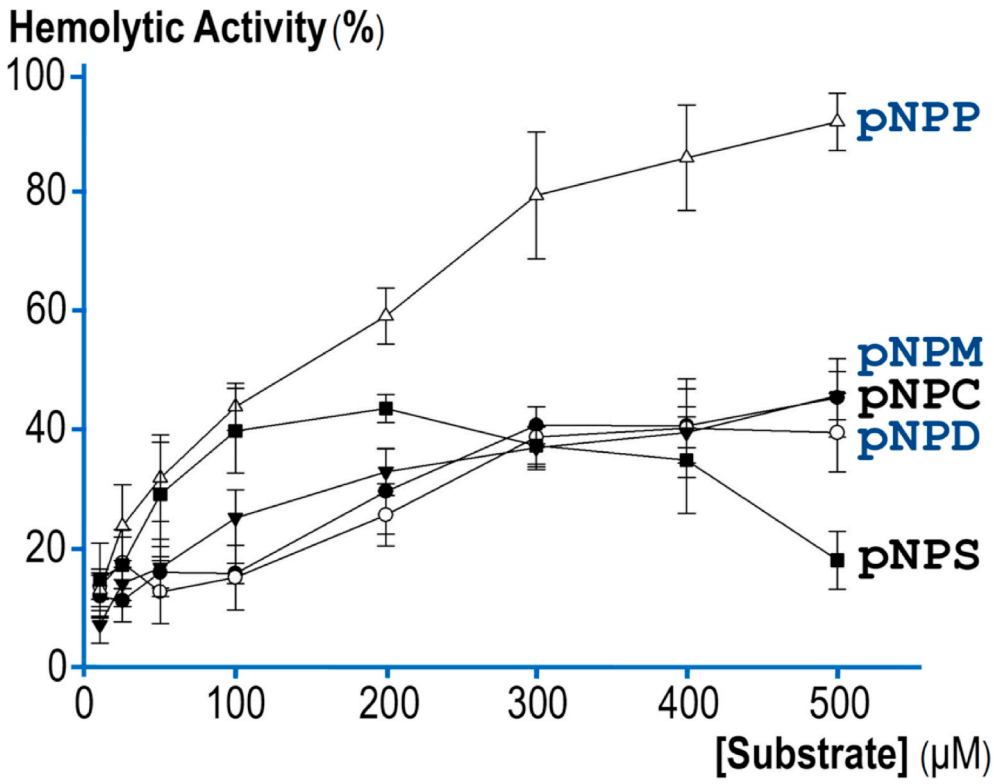

Fig. 2. Hemolytic activities of CyaA-Hly acylated *in vitro* by CyaC with various pNP-derivetive substrates, pNPC, $C_{8:0}$ (●), pNPD, $C_{10:0}$ (○), pNPM, $C_{14:0}$ (▼), pNPP, $C_{16:0}$ (Δ) and pNPS, $C_{18:0}$ (■). Error bars indicate standard errors of the mean from three independent experiments.

acyltransferase from pathogenic *E. coli* producing α-hemolysin (HlyA) that both myristoyl- and palmitoyl-ACPs are the most effective substrates for HlyC catalysis [28].

3.2. *Effects of acyl-chain lengths on CyaC-mediated CyaA-Hly activation and hence toxin-induced hemolysis*

Effects of such acyl-chain lengths on CyaC-acyltransferase activity was also comparatively studied *via* its relative enzymatic ability to modulate NA/CyaA-Hly *in vitro* to become hemolytically active against sheep erythrocytes. As the results shown in Fig. 2, when NA/CyaA-Hly was modulated by CyaC with pNPP substrate at ≥ 200 μM, the palmitoylated protein was revealed to be the most active (~90% hemolytic activity at 500 μM substrate) compared to four other acylated CyaA-Hly proteins. For instance, CyaA-Hly modified with myristoyl group through pNPM (another preferential substrate as shown above) appeared to exhibit only a half-maximal hemolytic activity (~45%) observed for palmitoylated CyaA-Hly. Nevertheless, it was previously shown that myristoyl-ACP but not palmitoyl-ACP conferred the highest hemolytic activity of the *E. coli* HlyA acylated *in vitro* by its activator (HlyC-acyltransferase) with a range of fatty acids (C_{12} to $C_{18:1}$) [28]. It should be noted that negative control reactions containing NA/CyaA-Hly incubated with only CyaC exhibited merely negligible activity (<5%), indicating the need of pNP substrates as mimics of the natural acyl-ACP donor.

Noted that LC-MS/MS analysis of a trypsin-digested fragment derived from palmitoylated CyaA-Hly (E^{972}GVA TQTTAYGK$_{C16:0}$$R^{984}$) confirmed the $C_{16:0}$ acylation of CyaA-Hly at Lys^{983} (*see* Supplementary Fig. S1). In line with this, it has very recently been shown that the ~180-kDa full-length CyaA toxin was exclusively activated *in vivo* to be hemolytically active through predominant modification of its Lys^{983} residue by C_{16} fatty acyl chains [29]. It is also noticeable that the stearylated-$C_{18:0}$ CyaA-Hly protein was found to display hemolytic activity similar to palmitoylated-$C_{16:0}$ CyaA-Hly when modulated with donor substrates at low concentrations (10-100 μM), but the stearylated CyaA-Hly-induced hemolysis became drastically reduced when the substrate concentrations were steadily increased from 200 to 500 μM (Fig. 2). A possible explanation for this observation is that in such high-concentration conditions (most likely above the critical micelle concentration, CMC), pNPS with its long hydrophobic acyl-chain ($C_{18:0}$) would be hardly soluble in the reaction buffer [20 mM Tris-HCl (pH 7.4), 150 mM NaCl and 5 mM $CaCl_2$] and more likely to become aggregated, thus decreasing a net number of free dissolved pNPS available for CyaC catalysis. It was previously observed for BSA-induced hydrolysis of pNP-acyl esters that the rate of esterolysis appeared to decrease with increasing chain length of the acyl moiety at concentrations above CMC (280 μM) [30].

It is worth mentioning that unlike our previous method for toxin activation *in vitro* [22], we herein were able to establish an *in vitro* modification system mediated by recombinant CyaC without the use of an acyl-ACP donor from its *E. coli*-host cell lysate. As also noted that CyaC-acyltransferase activity was measured indirectly through hemolytic activity of CyaA-Hly after being modulated with an appropriate acyl-donor substrate. Such observation at the highest hemolytic activity through the toxin modification by pNPP might be dependent on the net amount of palmitoylated toxins being formed and/or the physiological and biochemical features of the attached palmitoyl moiety. Accordingly, such results of CyaA-Hly activation *via* palmitoylation could suggest that pNPP is the most preferential substrate of CyaC-acyltransferase and the attached palmitoyl moiety ($C_{16:0}$) could possess the most proper acyl-chain length (~20 Å) for efficient membrane anchoring, and hence toxin-induced hemolysis. Being in agreement with this notion, our previous studies have shown that such toxin modification *via* Lys^{983}-palmitoylation was rather essential for stabilizing the toxin-induced ion-leakage pores [19].

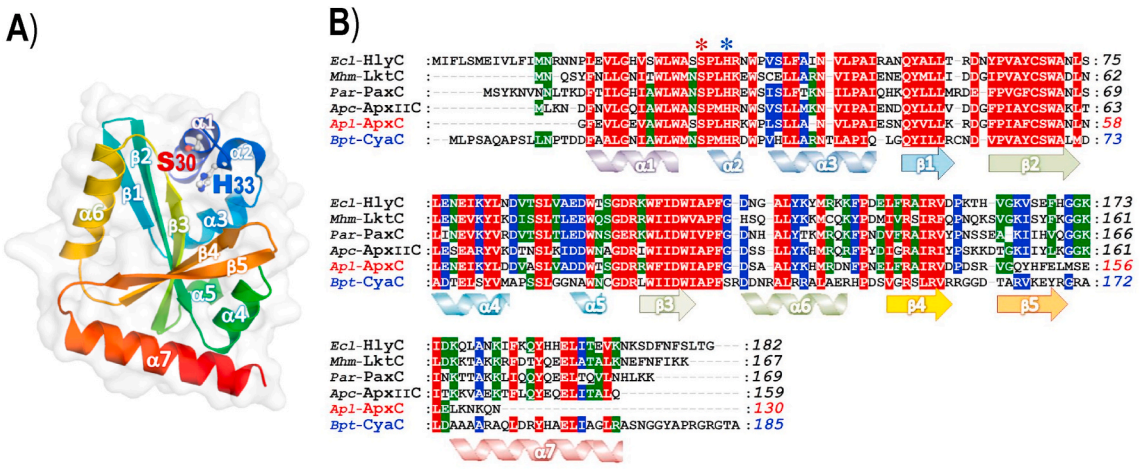

Fig. 3. (**A**) The CyaC modeled structure of which the ribbon diagram is rainbow-colored from purple at the N terminus to red at the C terminus. Residue numbers in the secondary structural elements are: α1 (Phe^{17} – Trp^{27}), α2 (Pro^{31} – Arg^{34}), α3 (Val^{38} – Gln^{50}), β1 (Gln^{53} – Arg^{58}), β2 (Val^{62} – Met^{72}), α4 (Ala^{74} – Met^{82}), α5 (Asn^{90} – Asn^{93}), β3 (Leu^{98} – Ile^{104}), α6 (Asp^{109} – Arg^{121}), β4 (Val^{126} – Arg^{133}), β5 (Thr^{138} – Arg^{147}) and α7 (Ala^{151} – Ser^{172}). Ball-and-stick models denote a proposed Ser^{30}-His^{33} catalytic dyad of CyaC. (**B**) Multiple sequence alignments of the deduced amino acid sequence of *Bpt*-CyaC, *B. pertussis* CyaC-acyltransferase (EF_592556) against those of *Apl*-ApxC, the ApxC crystal structure (PDB-4whn) from *Actinobacillus pleuropneumoniae* [25] and four other RTX-C acyltransferases, *i.e.*, *Ecl*-HlyC (*E. coli* hemolysin-acyltransferase, AJ488511.1), *Mhm*-LktC (*Mannheimia haemolytica* leukotoxin-acyltransferase, P55121), *Par*-PaxC (*Pasteurella aerogenes* PaxC-acyltransferase, U66588.1) and *Apc*-ApxIIC (*A. porcitonsillarum* ApxIIC-acyltransferase, Q5DI90) using ClustalX. *Bpt*-CyaC is used for denoting secondary structures according to the modeled structure shown in A. Amino acids are shaded red, blue and green to denote degrees of homology (6/6), (5/6) and (4/6), respectively. Proposed catalytic residues (*e.g.*, Ser^{30} and His^{33} for CyaC) are indicated by *. (For interpretation of the references to color in this figure legend, the reader is referred to the Web version of this article.)

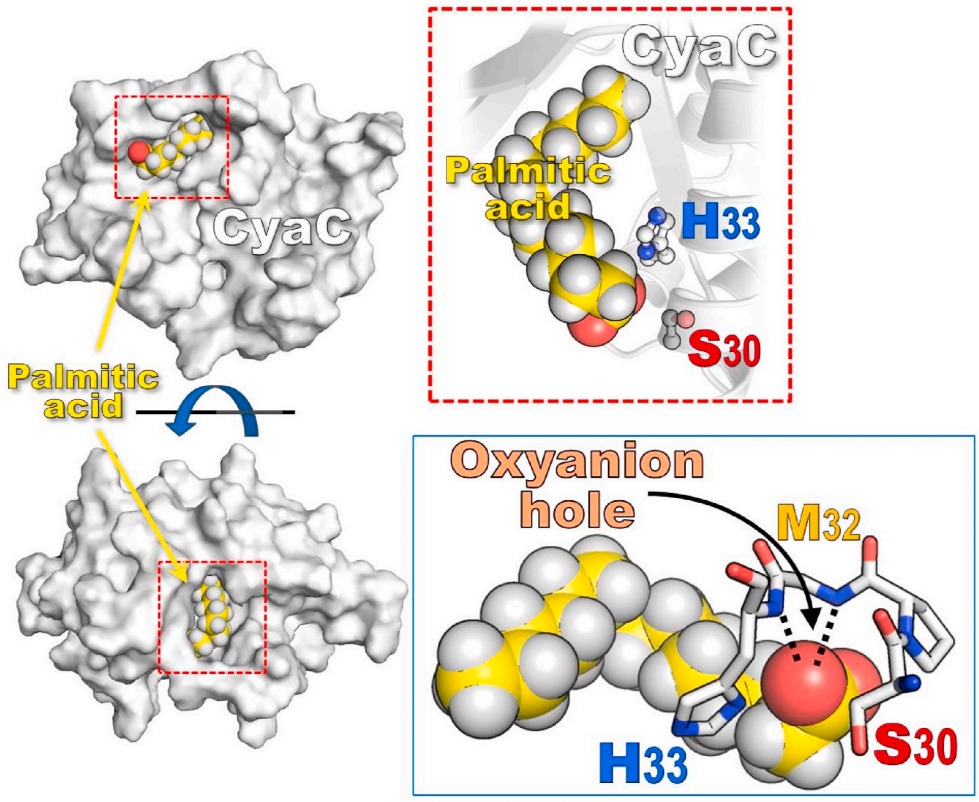

Fig. 4. Protein-ligand interactions between CyaC-acyltransferase and palmitic acid as depicted by surface representation and vdW spheres, respectively, showing that palmitic acid is buried in a hydrophobic cavity of the CyaC molecule. *Upper inset*, a zoom-in region demonstrating the position of palmitic acid's carboxyl group placed closely to the proposed Ser^{30}-His^{33} catalytic dyad. *Lower inset*, another zoom-in interaction region showing a putative oxyanion hole generated by an oxygen atom of ligand forming hydrogen bonds with backbone amide (NH) groups of Met^{32} and His^{33} from CyaC.

3.3. Ser^{30} and His^{33} could potentially serve as a catalytic dyad in CyaC-esterolysis of palmitoyl-donor substrate

Since no known structure of CyaC-acyltransferase has been elucidated yet, attempts were first made to construct a plausible 3D-modeled CyaC structure based on the ApxC crystal structure [25]. The resulting Ramachandran plot indicated that the CyaC modeled structure could remain in sterically favorable main-chain conformations (*see* Supplementary Fig. S2). As illustrated in Fig. 3A, the modeled structure comprises a single domain with a β-sheet core of five strands (β1, β2, β3, β4, and β5) connected by seven α-helices (α1, α2, α3, α4 α5, α6 and α7) to form a two-layer α/β sandwich similar to a classic fold of α/β hydrolase

Table 2
Kinetic parameters of CyaC wild-type and mutants with pNPP and corresponding effects on the hemolytic activity of CyaA-Hly[a].

Enzyme	V_{max} (U/mg)	k_{cat} (s^{-1})	K_M (mM)	k_{cat}/K_M ($s^{-1}mM^{-1}$)	Hemolytic activity (%)
Wt	$1.3 \times 10^3 \pm 39$	$4.7 \times 10^2 \pm 14$	0.34 ± 0.05	$1.4 \times 10^3 \pm 11$	88 ± 6.5
S30A	45 ± 0.3	16 ± 0.1	$7.0 \times 10^{-2} \pm 0.001$	$2.2 \times 10^2 \pm 7.0$	3.8 ± 4.7
H33A	68 ± 0.9	23 ± 0.3	$8.0 \times 10^{-2} \pm 0.003$	$2.8 \times 10^2 \pm 4.0$	4.5 ± 3.2

[a] Results were averaged from at least three independent experiments performed in duplicate. Both M-M and Lineweaver-Burk plots of individual corresponding data are shown in Supplementary Fig. S4.

family [31], with a potential catalytic dyad of Ser^{30} and His^{33} which are highly conserved among the RTX-acyltransferase family (*see* Fig. 3B). In analogy to the catalytic Cys-His dyad of several cysteine proteases [32,33], CyaC-His^{33} would serve as a general base catalyst, thus increasing the nucleophilicity of Ser^{30}.

When *in silico* docking was performed to gain greater insights into the architecture of CyaC interacting with its palmitoyl-donor substrate, the results illustrated in Fig. 4 revealed a high potential affinity of the CyaC molecule in binding to the docked palmitate ligand whose $C_{16:0}$-chain was found in a properly enclosed region within a relatively hydrophobic cavity of the modeled structure. In addition, the palmitate's carboxyl group appeared to be oriented outward, directly interacting with the two highly conserved Ser^{30} and His^{33} residues. As can be also inferred from the docked model that both conserved side-chains which possess functional groups for acyl-transfer catalysis (*i.e.*, hydroxyl group of Ser^{30} and unprotonated imidazole of His^{33}) were highly potent to get close in binding to the cleavage site on ligand molecule as both functional groups are only 3-4 Å from the ligand's carboxyl group (*see* Fig. 4, *upper inset*). Moreover, two adjacent backbone amide (NH) groups of Met^{32} and His^{33} could potentially form hydrogen bonds with a closet oxygen atom of the substrate, thus generating an oxyanion hole which would probably stabilize the tetrahedral intermediate formed during catalysis (*see* Fig. 4, *lower inset*). This hole which is commonly described in many bacterial enzyme structures (*e.g.*, esterase and acyltranferase) [34,35] could allow for positioning of such a substrate, which would suffer from steric hindrance if it could not occupy the hole.

To test our notion from the docking data, two CyaC mutants (*i.e.*, S30A and H33A) of which Ser^{30} and His^{33} were replaced individually with Ala were initially determined for their esterolytic activity against pNPP substrate in comparison with the wild-type (Wt) enzyme. As can be seen in Table 2, both Ala-substitutions critically affected the CyaC esterolytic activity in all kinetic aspects. Among the kinetic parameters obtained, Vmax appeared to be mostly affected by both mutations as it decreased by about 20–30 fold in each corresponding mutant compared to that of Wt. The S30A and H33A mutations also decreased K_M values, suggesting an increase in binding affinity for the pNPP substrate, however, the greatest impact of the two mutations is the 20-30 fold reduction in turnover (*see* Table 2). Consequently, their k_{cat}/K_M values were found greatly reduced, thus clearly indicating an adverse influence of these mutations on catalytic efficiency of CyaC and hence an importance of Ser^{30} and His^{33} that would serve as a potential catalytic dyad in CyaC-esterolytic catalysis.

Experiments were further conducted to determine an effect of such Ala-substitutions on CyaC-acylation activity toward the resulting hemolytic activity of activated CyaA-Hly. Consistent with observations from the CyaC-esterolysis assay, NA/CyaA-Hly proteins after being mediated by each CyaC mutant displayed an almost entire loss of corresponding hemolytic activity (*see* Table 2). Such a drastic decrease in CyaA-Hly-induced hemolysis was likely due to incapability of each CyaC

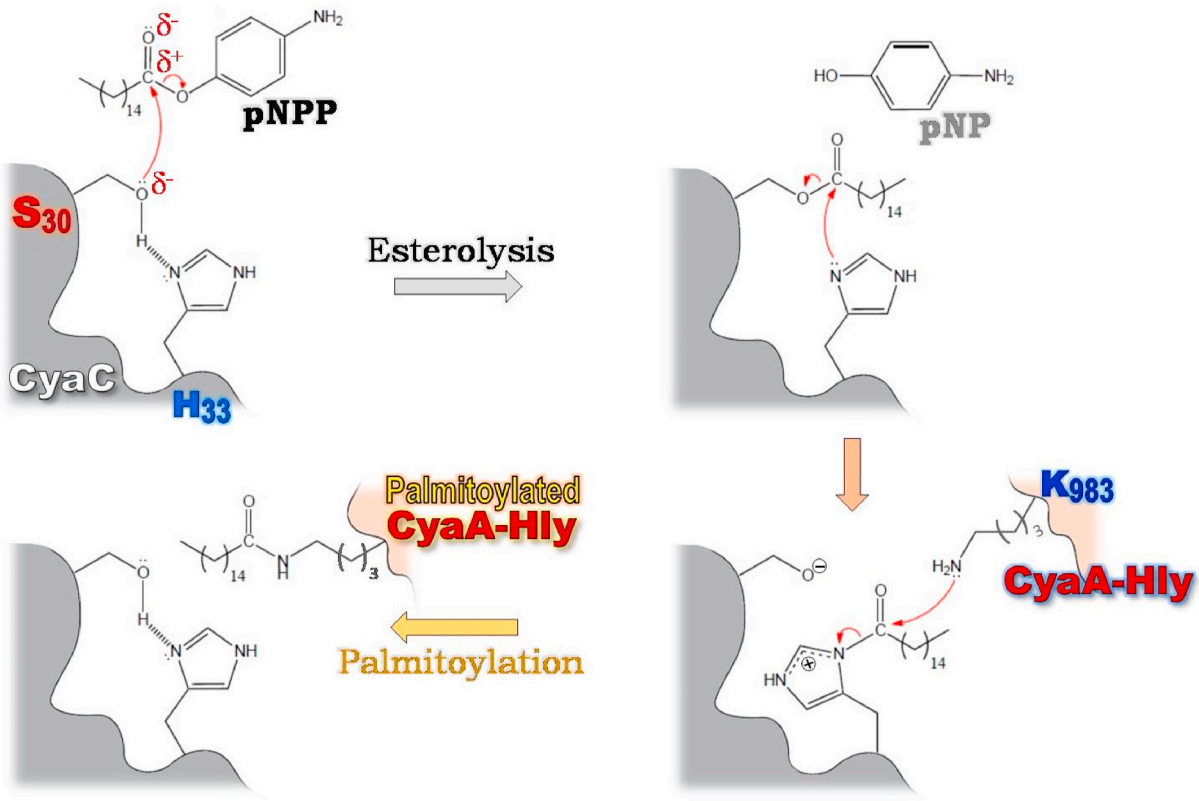

Fig. 5. A putative catalytic mechanism involving roles of both Ser^{30} and His^{33} residues that could potentially act as a nucleophile-activation dyad in CyaC-acyltransferase esterolysis of acyl-donor substrate, *e.g.* pNPP, as well as toxin activation through preferential palmitoylation at Lys^{983} of NA/Cya-HlyA.

mutant to palmitoylate NA/CyaA-Hly as verified by LC-MS/MS analysis revealing no palmitoyl moiety being conjugated at Lys^{983} of CyaA-Hly. These results suggested that Ser^{30} and His^{33} would play a crucial role in CyaC-directed NA/CyaA-Hly palmitoylation *in vitro* and hence toxin-induced hemolysis. Taken together, all these independent assays consistently signified that both Ser^{30} and His^{33} residues could potentially act as a nucleophile-activation dyad in CyaC-acyltransferase esterolysis of acyl-donor substrates as well as NA/Cya-HlyA acylation through CyaC-catalyzed preferential palmitoylation as its putative catalytic mechanism is illustrated in Fig. 5. Unlike other previous studies for HlyC-directed pro-HlyA acylation [36,37], our present findings evidently revealed that a natural acyl-ACP donor appeared not to be a strict requirement for such CyaC-mediated NA/Cya-HlyA acylation *in vitro*, possibly implicating an alternative post-translational modification of CyaA-Hly underlining RTX-toxin maturation *in vivo*.

Acknowledgment

This work has been generously supported by grants from Thailand Science Research and Innovation (MRG-59-8-0040), Burapha University and Mahidol University.

Appendix A. Supplementary data

Supplementary data to this article can be found online at https://doi.org/10.1016/j.abb.2020.108615.

References

[1] N.H. Carbonetti, G.V. Artamonova, C. Andreasen, N. Bushar, Pertussis toxin and adenylate cyclase toxin provide a one-two punch for establishment of *Bordetella pertussis* infection of the respiratory tract, Infect. Immun. 73 (2005) 2698–2703.
[2] P. Glaser, H. Sakamoto, J. Bellalou, A. Ullmann, A. Danchin, Secretion of cyclolysin, the calmodulin-sensitive adenylate cyclase-haemolysin bifunctional protein of *Bordetella pertussis*, EMBO J. 7 (1988) 3997–4004.
[3] M.J. Bart, S.R. Harris, A. Advani, Y. Arakawa, D. Bottero, V. Bouchez, P. K. Cassiday, C.-S. Chiang, T. Dalby, N.K. Fry, et al., Global population structure and evolution of *Bordetella pertussis* and their relationship with vaccination, mBio 5 (2014), e01074.
[4] J.M. Warfel, L.I. Zimmerman, T.J. Merkel, Acellular pertussis vaccines protect against disease but fail to prevent infection and transmission in a nonhuman primate model, Proc. Natl. Acad. Sci. U.S.A. 111 (2014) 787–792.
[5] A. Lim, J.K. Ng, C. Locht, S. Alonso, Protective role of adenylate cyclase in the context of a live pertussis vaccine candidate, Microb. Infect. 16 (2014) 51–60.
[6] A. Malik, C. Imtong, N. Sookrung, G. Katzenmeier, W. Chaicumpa, C. Angsuthanasombat, Structural characterization of humanized nanobodies with neutralizing activity against the *Bordetella pertussis* CyaA-hemolysin: implications for a potential epitope of toxin-protective antigen, Toxins 8 (2016) 99–111.
[7] P. Guermonprez, N. Khelef, E. Blouin, P. Rieu, P. Ricciardi-Castagnoli, N. Guiso, D. Ladant, C. Leclerc, The adenylate cyclase toxin of *Bordetella pertussis* binds to target cells via the alpha(M)beta(2) integrin (CD11b/CD18), J. Exp. Med. 193 (2001) 1035–1044.
[8] P. Gueirard, A. Druilhe, M. Pretolani, N. Guiso, Role of adenylate cyclase-hemolysin in alveolar macrophage apoptosis during *Bordetella pertussis* infection *in vivo*, Infect. Immun. 66 (1998) 1718–1725.
[9] R. Osicka, A. Osickova, S. Hasan, L. Bumba, J. Cerny, P. Sebo, *Bordetella* adenylate cyclase toxin is a unique ligand of the integrin complement receptor 3, Elife 4 (2015), e10766.
[10] O. Knapp, E. Maier, G. Polleichtner, J. Masin, P. Sebo, R. Benz, Channel formation in model membranes by the adenylate cyclase toxin of *Bordetella pertussis*: effect of calcium, Biochemistry 42 (2003) 8077–8084.
[11] B. Powthongchin, C. Angsuthanasombat, Effects on haemolytic activity of single proline substitutions in the *Bordetella pertussis* CyaA pore-forming fragment, Arch. Microbiol. 191 (2009) 1–9.
[12] C. Kurehong, C. Kanchanawarin, B. Powthongchin, G. Katzenmeier, C. Angsuthanasombat, Membrane-pore forming characteristics of the *Bordetella pertussis* CyaA-hemolysin domain, Toxins 7 (2015) 1486–1496.
[13] C. Kurehong, C. Kanchanawarin, B. Powthongchin, P. Prangkio, G. Katzenmeier, C. Angsuthanasombat, Functional contributions of positive charges in the pore-lining helix 3 of the *Bordetella pertussis* CyaA-hemolysin to hemolytic cctivity and ion-channel opening, Toxins 9 (2017) 109–121.
[14] G.D. Westrop, E.K. Hormozi, N.A. Da Costa, R. Parton, J.G. Coote, *Bordetella pertussis* adenylate cyclase toxin: proCyaA and CyaC proteins synthesised separately in *Escherichia coli* produce active toxin *in vitro*, Gene 180 (1996) 91–99.
[15] M. Hackett, L. Guo, J. Shabanowitz, D.F. Hunt, E.L. Hewlett, Internal lysine palmitoylation in adenylate cyclase toxin from *Bordetella pertussis*, Science 266 (1994) 433–435.
[16] T. Basar, V. Havlicek, S. Bezouskova, M. Hackett, P. Sebo, Acylation of lysine 983 is sufficient for toxin activity of *Bordetella pertussis* adenylate cyclase. Substitutions of alanine 140 modulate acylation site selectivity of the toxin acyltransferase CyaC, J. Biol. Chem. 276 (2001) 348–354.
[17] R. Benz, E. Maier, D. Ladant, A. Ullmann, P. Sebo, Adenylate cyclase toxin (CyaA) of *Bordetella pertussis*; Evidence for the formation of small ion-permeable channels and comparison with HlyA of *Escherichia coli*, J. Biol. Chem. 269 (1994), 27231-27139.
[18] J. Masin, M. Basler, O. Knapp, M. El-Azami-El-Idrissi, E. Maier, I. Konopasek, R. Benz, C. Leclerc, P. Sebo, Acylation of lysine 860 allows tight binding and cytotoxicity of *Bordetella* adenylate cyclase on CD11b-expressing cells, Biochemistry 44 (2005) 12759–12766.
[19] K. Meetum, C. Imtong, G. Katzenmeier, C. Angsuthanasombat, Acylation of the *Bordetella pertussis* CyaA-hemolysin: functional implications for efficient membrane insertion and pore formation, Biochim. Biophys. Acta Biomembr. 1859 (2017) 312–318.
[20] V. Raksanoh, P. Prangkio, C. Imtong, N. Thamwiriyasati, K. Suvarnapunya, L. Shank, C. Angsuthanasombat, Structural requirement of the hydrophobic region of the *Bordetella pertussis* CyaA-hemolysin for functional association with CyaC-acyltransferase in toxin acylation, Biochem. Biophys. Res. Commun. 499 (2018) 862–867.
[21] P. Stanley, V. Koronakis, C. Hughes, Acylation of *Escherichia coli* hemolysin: a unique protein lipidation mechanism underlying toxin function, Microbiol. Mol. Biol. Rev. 62 (1998) 309–333.
[22] N. Thamwiriyasati, B. Powthongchin, J. Kittiworakarn, G. Katzenmeier, C. Angsuthanasombat, Esterase activity of *Bordetella pertussis* CyaC-acyltransferase against synthetic substrates: implications for catalytic mechanism *in vivo*, FEMS Microbiol. Lett. 304 (2010) 183–190.
[23] B. Powthongchin, C. Angsuthanasombat, High level of soluble expression in *Escherichia coli* and characterisation of the CyaA pore-forming fragment from a *Bordetella pertussis* Thai clinical isolate, Arch. Microbiol. 189 (2008) 169–174.
[24] Q. Wang, J.C. Allen, H.E. Swaisgood, Binding of vitamin D and cholesterol to beta-lactoglobulin, J. Dairy Sci. 80 (1997) 1054–1059.
[25] N.P. Greene, A. Crow, C. Hughes, V. Koronakis, Structure of a bacterial toxin-activating acyltransferase, Proc. Natl. Acad. Sci. U.S.A. 112 (2015) E3058–3066.
[26] P. Benkert, S.C. Tosatto, D. Schomburg, QMEAN: a comprehensive scoring function for model quality assessment, Proteins 71 (2008) 261–277.
[27] A. Grosdidier, V. Zoete, O. Michielin, SwissDock, a protein-small molecule docking web service based on EADock DSS, Nucleic Acids Res. 39 (2011) W270–W277.
[28] J.P. Issartel, V. Koronakis, C. Hughes, Activation of *Escherichia coli* prohaemolysin to the mature toxin by acyl carrier protein-dependent fatty acylation, Nature 351 (1991) 759–761.
[29] A. Osickova, H. Khaliq, J. Masin, D. Jurnecka, A. Sukova, R. Fiser, J. Holubova, O. Stanek, P. Sebo, R. Osicka, Acyltransferase-mediated selection of the length of the fatty acyl chain and of the acylation site governs activation of bacterial RTX toxins, J. Biol. Chem. 295 (2020). https://www.jbc.org/cgi/doi/10.1074/jbc.RA120.014122.
[30] H. Østdal, H.J. Andersen, Non-enzymic protein induced hydrolysis of *p*-nitrophenyl acyl esters in relation to lipase/esterase assays, Food Chem. 55 (1996) 55–61.
[31] M. Holmquist, Alpha/beta-hydrolase fold enzymes: structures, functions and mechanisms, Curr. Protein Pept. Sci. 1 (2000) 209–235.
[32] A. Paasche, A. Zipper, S. Schäfer, J. Ziebuhr, T. Schirmeister, B. Engels, Evidence for substrate binding-induced zwitterion formation in the catalytic Cys-His dyad of the SARS-CoV main protease, *B*iochemistry 53 (2014) 5930–5946.
[33] S. Saraswat, M. Chaudhary, D. Sehgal, Hepatitis E virus cysteine protease has papain-like properties validated by *in silico* modeling and cell-free inhibition assays, Front Cell Infect Microbiol 9 (2020), https://doi.org/10.3389/fcimb.2019.00478.
[34] L.-C. Lee, Y.-L. Lee, R.-J. Leu, J.-F. Shaw, Functional role of catalytic triad and oxyanion hole-forming residues on enzyme activity of *Escherichia coli* thioesterase I/protease I/phospholipase L1, Biochem. J. 397 (2006) 69–76.
[35] A. Röttig, A. Steinbüchel, Acyltransferases in bacteria, Microbiol. Mol. Biol. Rev. 77 (2013) 277–321.
[36] M.S. Trent, L.M. Worsham, M.L. Ernst-Fonberg, The biochemistry of hemolysin toxin activation: characterization of HlyC, an internal protein acyltransferase, Biochemistry 37 (1998) 4644–4652.
[37] P. Stanley, V. Koronakis, C. Hughes, Acylation of *Escherichia coli* hemolysin: a unique protein lipidation mechanism underlying toxin function, Microbiol. Mol. Biol. Rev. 62 (1998) 309–333.